Hydronic configurations of hybrid heat production systems in buildings : general design methodology and case studies

Reference:
Van Riet Freek, Verhaert Ivan.- Hydronic configurations of hybrid heat production systems in buildings : general design methodology and case studies
Applied thermal engineering: design, processes, equipment, economics - ISSN 1359-4311 - 164(2020), UNSP 114454
Full text (Publisher's DOI): https://doi.org/10.1016/J.APPLTHERMALENG.2019.114454
To cite this reference: https://hdl.handle.net/10067/1626180151162165141

Hydronic configurations of hybrid heat production systems in buildings: general design methodology and case studies

Freek Van Riet[a,*], Ivan Verhaert[a]

[a] *University of Antwerp, EMIB research group, Groenenborgerlaan 171, B-2020 Antwerp, Belgium*

Abstract

Hybrid heat production systems, in which sustainable technologies such as Combined Heat and Power (CHP) or heat pumps are combined with auxiliary heaters, have the potential to increase energy efficiency in buildings. In order to exploit this potential, a proper hydronic configuration of the production system is of uttermost importance. Unfortunately, both scientific literature and design guides have focussed little on this aspect.

Therefore, this paper proposes a general simulation-based design methodology for selecting the hydronic configuration of a hybrid production system. To illustrate the methodology, it is applied on different case studies in which either a CHP or an Electrical ground-coupled Heat Pump (EHP) is assisted by an auxiliary boiler. The considered apartment building is equipped with a collective heating system for both space heating and domestic hot water (DHW) production, and four different combinations of the temperature levels are considered.

Results show that if a CHP is considered, the auxiliary boiler should be implemented in parallel and be assisted by a modulating valve: this increases the Relative Primary Energy Savings (RPES) with up to 6.2 percentage points. EHPs require a separate circuit in the production system for space heating and DHW, preferably with preheating of the domestic cold water (an increase in RPES of up to 16.1 percentage points was reported).

The use of a new type of Load Duration Curve to analyse the simulation results proved to be a comprehensible measure for decision making at the level of every stakeholder in the design process. In conclusion, the proposed methodology can assist these stakeholders in their pursuit of high performance hybrid heat production systems.

Keywords: Hydronic configurations, Hybrid heat production, Cogeneration, CHP, Ground-coupled heat pumps, GCHP

1. Introduction

1.1. Problem statement

Energy-efficiency is a strict requirement to reach the 2020 and 2030 climate-related goals in Europe [1]. Not surprisingly, over the past decades the integration of sustainable heat production in buildings has been increasing [2, 3, 4]. This integration is facilitated by the trend towards collective heating systems[1], as the used technologies are subject to economies of scale [5, 6]. For large buildings, two technologies in particular are wide-spread: Internal Combustion Engine-based Combined Heat and Power (ICE-CHP, from here also referred to as just CHP) [7, 8] and Electric ground-coupled Heat Pumps (EHP) [9, 10].

The disadvantage of both technologies is their capital cost, and therefore, if one of them is implemented in a building it is often combined with an inexpensive auxiliary heater, typically a boiler. This boiler assists

*Corresponding author: freek.vanriet@uantwerpen.be

[1] In 'collective heating systems' multiple residences are served by a single production system

the sustainable producer (from here also referred to as 'principal heat producer') at peak load conditions, allowing the size of the latter to be reduced [11, 12, 13].

Such *hybrid heat production systems* are highly complex to design and require guides for a proper integration in buildings [14, 15, 16, 17, 18]. While the steps in these guides are described differently, all have a common structure (also summarized in Figure 1, see black text):

- Quantify the heat load demand of the building and, if a CHP is considered, the electric load demand. When renovating buildings, these profiles can be obtained by measurements or estimated by data provided by energy suppliers. For new buildings, profiles based on either 'standard' buildings or simulations can be used.
- With these profiles and after performing a (pre-) feasibility study, the actual design concept is developed. The following aspects should be covered: technology selection, sizing (including of an auxiliary heater and thermal storage tank), determining the control strategy and choosing the hydronic configuration.
- Finally, the design is translated into a real installation in the realisation phase, and is afterwards operated and maintained.

Great efforts have been made to develop methodologies for the different aspects of the design of hybrid heat production systems. Pragmatic approaches exist, which allow simplistic but fast sizing, without the need for intensive computations: e.g. the maximum rectangle method [19] maximises the thermal production of a CHP that is not able to operate in part load, and a corresponding thermal storage tank can be sized to limit the number of ON/OFF cycles in a day [14]. Analogue approaches exists for heat pump sizing (based on a 'β-curve') and corresponding tank sizing to limit the number of shut-downs [17, 18]. Also detailed, more computationally expensive methodologies have been proposed for hybrid heat production systems, whether or not including electricity or cold production. Indeed, numerous (multi-objective) optimisation algorithms can be found in literature that are developed for technology selection and sizing of the components [20, 11, 21, 22, 23, 6, 24, 25, etc.]. Furthermore, various authors have reported methodologies to optimise operation strategies [26, 27, 28, 29, 23, 30, 31, 32, etc.]

Given the selected technologies, the sizes of all production components and the strategy to control them, a final question remains: how should all components be connected by pipes, pumps and valves? It is known that in practice this has an important effect on the performance of the production system [4]. Unfortunately, current guides [14, 15, 16, 17, 18, 33] hardly provide an answer to the question, or lack consistency and scientific proof. Also in academics, the design of the hydronic configuration of hybrid heat production systems is only in its infancy. The few scientific references that are available are discussed hereafter.

Glembin et al. [34] investigated five different configurations of a hybrid system with solar collectors and a boiler, providing heat for space heating and domestic hot water (DHW) production of a single-family house. A difference in energy savings of up to 12 percentage points between the different configurations was found[2]. The capacity and type (with or without improvement of the stratification) of thermal storage tank were different between the different hydronic configurations.

Other research [35] compared multiple configurations of solar collectors with either a heat pump or a boiler, also for a single-family house with both space heating and DHW production. Along with the hydronic configurations of the production system, the types of emitters were altered (radiators, floor heating or concrete core activation), which revealed differences with the same order of magnitude: assuming, respectively, a heat pump or a boiler as auxiliary heater, up to 12% or 11% less energy was consumed[3].

Bonabe de Rougé et al. [36] investigated three different hydronic configurations for a hybrid heating system consisting of a Stirling engine-based CHP and a boiler: a difference in relative energy savings of up to 6 percentage points[4] was found for a single-family house with both space heating and DHW. All three

[2]Estimated based on Fig. 2 of reference [34] and considering the case with a collector area of $30m^2$

[3]Estimated based on, respectively, Fig. 2 and 3 of reference [35], and considering a collector area of $60m^2$ and the cases with radiators as emitters.

[4]Estimated based on Fig. 7 of reference [36] for "Low" occupancy profiles of concepts "C1 160" and "C2 750".

hydronic configurations were, beside the difference in configuration itself, characterised by other storage tank capacities and insulation levels.

For a hybrid production system with an ICE-CHP, different hydronic concepts were compared ('serial', 'parallel' and 'shunt' connections between CHP and boiler) and showed a difference of up to 10 percentage points of relative energy savings [37, 38]. These differences were found to be even more expressed for hybrid production systems with an EHP and a boiler (up to 20 percentage points [39]). The latter three papers considered an apartment building with a collective system for space heating only; domestic hot water (DHW) was not considered.

Within the limited literature available on hydronic configurations of hybrid heat production systems, three main problems can be identified:

1. None of the literature describes a methodology that provides a comprehensible output which can be used for decision making of a design process by all stakeholders: installers, engineering offices and manufacturers. The susceptibility of the performance of hybrid heat production systems to the hydronic configuration, and its complexity that installers, engineering offices and manufacturers have to deal with, highlight the need for a methodology which is more comprehensible for its users.
2. Most research fails to distinguish between the effect of the actual hydronic configuration and other design choices, such as tank characteristics (type, number, size or insulation level) or type of emitter systems. In other words, the results allow to observe mixed effects only, which complicate the design process if some boundary conditions of the hydronic configuration selection are determined in advance. This is especially true when different stakeholders are responsible for different aspects of the design.
3. Not a single case is covered in which a hybrid heat production system with either one of the two most common sustainable technologies for large buildings (an EHP or an ICE-CHP) serves a collective heating system for both space heating and domestic hot water. Such a common combination requires a thorough analysis.

1.2. Scope and outline of the paper

This paper proposes a general methodology to design the hydronic configuration of a hybrid heat production system, consisting of a 'principal' and an 'auxiliary' heat producer, and applies it on different case studies to formulate generalised guidelines. The paper thereby provides a significant contribution to the research field of hybrid heat production systems at three levels, covering the main problems identified above.

First of all, a design methodology is proposed consisting of three steps (Section II): the development of a morphological chart, simulation-based evaluation and the actual selection of an hydronic configuration. Also a new type of 'extended Load Duration Curve' is suggested which enables a comprehensible analysis for decision making (solution to problem 1).

While the different steps of the proposed design methodology, including the developed simulation environment and type of Load Duration Curve, can be used for different types of heating systems, here (Section III) it is applied to the most common hybrid production systems for collective housing. More specific, eight representative case studies are considered, all consisting of an apartment building with a collective system for both space heating and DHW production. Four cases are equipped with an ICE-CHP and the other four with a ground-coupled heat pump. For both groups, the four cases are characterised by different design temperature levels of the space heating and DHW circuit. In combination with an in-depth analysis of the dynamic behaviour of all configurations, this sensitivity analysis allows to formulate generalised guidelines that can be consulted by designers (solution to problem 2). Within the analysis of each case study, the boundary conditions are kept the same for each hydronic configurations to prevent the results from reflecting mixed effects (solution to problem 3).

The formulated guidelines are not only useful for the stakeholders of design processes, they also allow academic researchers to select only a single hydronic configuration so that other aspects, such as technology selection, sizing or control strategy, can be investigated.

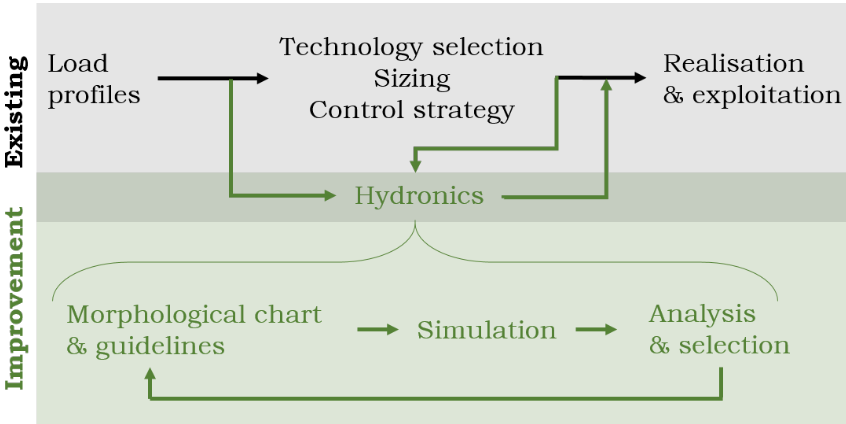

Figure 1: Schematic representation of the design methodology proposed in this research (in green), given in the context of existing methodologies (black).

2. Design methodology

2.1. General description

Figure 1 shows both the existing methodologies, as discussed in the introduction, and the proposed improvement. Existing methodologies result, in general, in the following outputs that are required for designing the hydronic configuration of an hybrid production system:

- Demand side[5]-specific boundary conditions: the type of heat distribution system, characteristics of emitter system, inhabitant behaviour and thermo-physical properties of the building itself. All these characteristics are determined in an earlier stage of the design process and are translated into representative load profiles of the demand side, referred to as Demand Load Profiles (DLPs).

- Production-specific boundary conditions: selected heat production technologies, their respective sizes and control strategies. These decisions are based on existing optimisation strategies that take the Demand Load Profiles (DLPs) as input. Ideally, these DLPs contain not only the thermal load of the building in time, but also at which temperature this load is required. This allows to take the limited temperature range of e.g. heat pumps into account. The outputs of the optimisation consist typically of, beside the decisions themselves, the heat loads of each component in the production system at each time step. These 'Production Load Profiles' (PLPs) reflect the expected behaviour of the production system for the given production-specific boundary conditions, while making abstraction of the hydronic configuration. Indeed, the optimisation is typically based on loads only, not on detailed simulations of the hydronics.

Given the load profiles (both DLP and PLP) and the boundary conditions as starting point (see two green arrows towards 'Hydronics' in Figure 1), the methodology follows three steps in order to arrive at an hydronic configuration.

First, a structured representation of existing and/or novel hydronic configurations is given by means of a morphological chart and corresponding guidelines. In the next subsection, this is given for hybrid production system with either a CHP or an EHP that serve a collective heating system for both space heating and domestic hot water (DHW) production. After that, each hydronic configuration is simulated based on dynamic building system simulations (Subsection 2.3). Then, based on the results of these simulations, the new type of Load Duration Curves (LDCs) are generated for all the hydronic configurations, thereby

[5]In this paper, the term 'demand side' refers to the heat distribution system, emitters and the building itself, i.e everything that is not included in the 'heat production system'

providing a graphical tool for analysis and selection (Subsection 2.4). After these three steps, insights for other novel configurations or the formulation of new guidelines can provide feedback for future projects or for the current project (reversed arrow in Figure 1).

2.2. Morphological chart and guidelines

As already discussed in the introduction, literature -scientific literature in particular- lacks information on hydronic designs of heat production systems. Therefore, this subsection is based on input from different parties in the private sector involved in the design of hybrid heat production systems. Based on this input, the current practice of hybrid heat production systems applied to collective systems for space heating and domestic hot water production was defined, with a focus on either ICE-CHPs or EHPs.

To set up a morphological chart, the functionality of each component should be specified:

- the 'principal heat producer', i.e. the CHP or EHP, serves as sustainable heat source.
- a storage tank (from here referred to as just 'tank') balances the heat produced by the principal heat producer and the building's thermal demand. Depending on its state of charge, as quantified by temperature measurements, and assuming a heat-lead control it generates an ON/OFF signal for the principal heat producer.
- the 'auxiliary heat producer', i.e. the boiler, serves as a peak load heat producer. It controls the supply water temperature if it does not reach its set point.
- the distribution system transfers heat from the production system to the end use. This distribution system contains a tank with DHW to reduce peak loads of DHW production (from here referred to as just 'DHW tank').
- The end use consists of heat emitters and tapping units to transfer heat for space heating or to provide DHW.

Each of these required functionalities can have multiple solutions (i.e. hydronic configurations), which are presented in a morphological chart for configurations with either CHP or EHP in Figure 2. The different solutions are represented by a set of five *Base Circuits* (BCs), a concept which was introduced by Vandenbulcke [40] for the evaluation of thermal distribution systems. In total, seven hydronic configurations (HC) are considered: from 'HC I' to 'HC VI' with two variations regarding control strategy for 'HC II'. Not all configurations are applicable for both CHP and EHP, and for those that are, a small difference in design exists: the presence of a three-way valve in the CHP BC and Tank BC. Before all configurations are discussed, these two differences will be explained.

First, ICE-CHPs are equipped with an internal cooling circuit to recuperate heat and in order to obtain proper operation (high electrical efficiency). For this latter reason, the temperature of the internal cooling circuit fluid going in the engine block is restricted to a minimum of typically 60°C. While other methods exist, the most conventional way to achieve this restriction is by control of the inlet water temperature [38]. Therefore, the considered CHP devices are equipped with a modulating three-way valve (see PHP BCs in Figure 2 for configurations with a CHP).

Second, heat pumps are even more sensitive to the temperature they operate and shut down if an upper limit is exceeded. To avoid this, an open-closed three-way valve (see Tank BCs in Figure 2 for configurations with an EHP) prevents return water at a too high temperature to flow towards the heat pump or to flow into the tank.

From here, all hydronic configurations (HC) of the production system will be discussed all serving the same building. The exact demand- and production-specific boundary conditions are discussed further in Subsection 3.1 . Note that the principle of HC I and the two variations of HC II have been discussed before [39, 38].

- **HC I**. The boiler is integrated in series with the supply water. If it is OFF, water is bypassed by a three-way valve. Note that the boiler inlet water is heated by the principal heat producer, which decreases the boiler's efficiency.

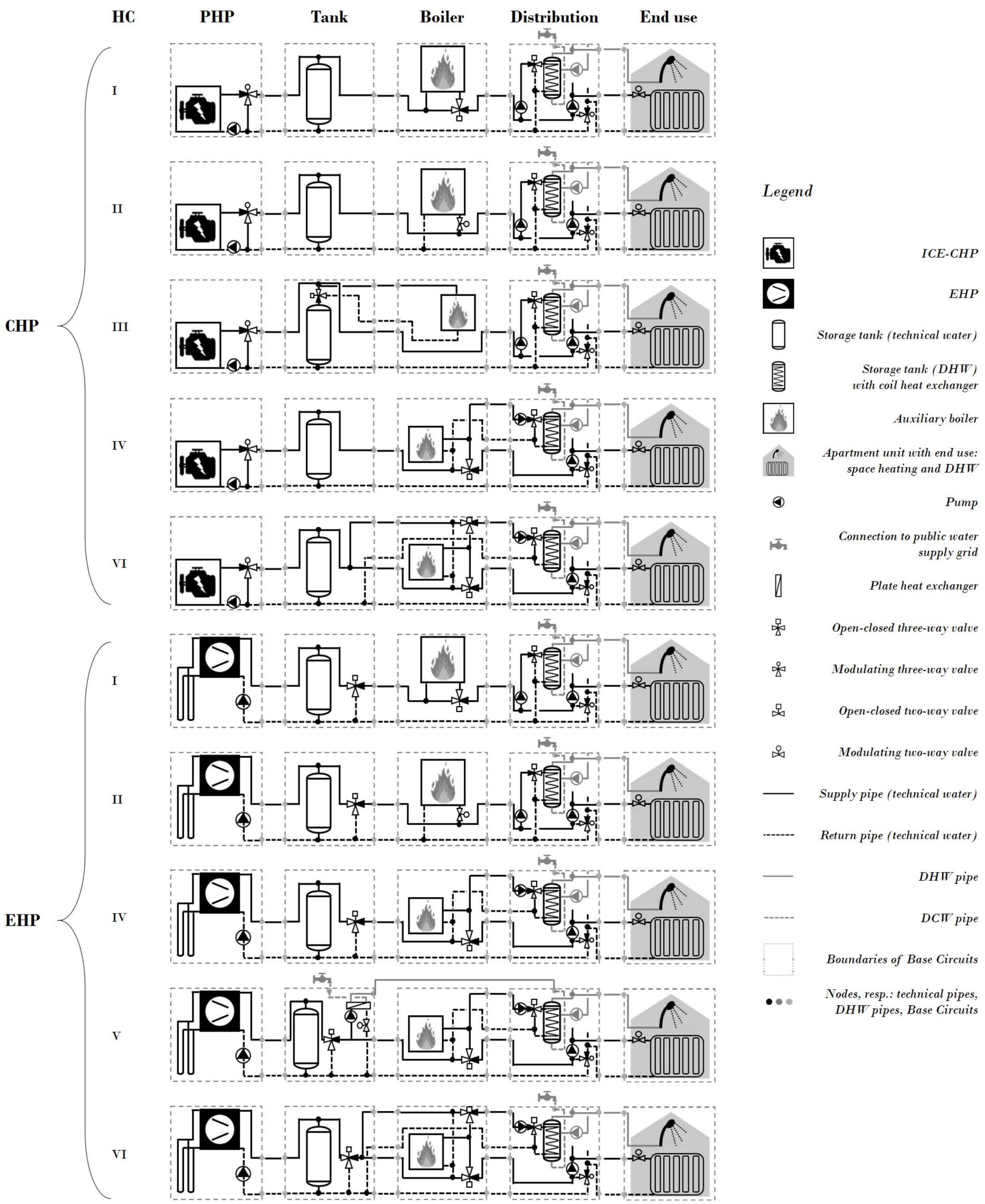

Figure 2: Morphological chart of the production system for two different Principal Heat Producers (PHP). It is intended to show the basics of the hydronic configurations, not as a P&ID. Indeed, non-return valves and balancing valves are not shown.

- **HC II**. A lower inlet temperature can be achieved if the boiler is implemented in parallel with the principal heat producer. Again, if the boiler is ON, the amount of water that flows through it depends on the control strategy of the two-way valve:
  - Open-closed control valve (referred to as '**HC IIo/c**'): if the valve opens, it always opens completely and a fixed share of the return water flows directly through the boiler; the other share flows towards the tank. The ratio between these two shares is ensured by balancing valves which settings depend on the ratio of the nominal boiler and PHP heat load. The disadvantage of this control is that it decreases the flow towards the tank which is then discharged at a lower rate. In turn, this might decrease the operation of the principal heat producer since the latter is shut down if the tank is charged completely.
  - By using a modulating valve (referred to as '**HC IImod**'), the decreased discharging rate can be minimised while taking overheating of the boiler into account at low flow rates [39, 38]. This modulating valve also prevents flow through the tank if the tank is not able to provide net heat. This might temporarily occur if the temperature of return water is higher than that of the water in the tank.
- **HC III**. Analogue to HC II with modulating valve control, also this configuration aims to combine a low boiler inlet temperature, while preventing the tank from being discharged at a low rate. This is possible by integrating the boiler above the tank, so that the flow through the tank is not affected by the operational state of the boiler. Note that this configuration is only able to increase temperature of the supply water if water flows through the tank from bottom to top. For cases with a CHP with inlet temperature control, this is acceptable since also the outlet temperature is high (typically 80 °C). For cases with heat pumps this might result in malfunctioning since the supply temperature cannot be guaranteed if the water in the tank flows from top to bottom. As a result, this configuration is not considered for cases with an EHP.
- **HC IV**. To exploit a potential difference in temperature requirements between space heating and DHW, both types of end uses are heated with a separate circuit. While especially for heat pumps this configuration is expected to be beneficial, it is also considered for cases with a CHP. The disadvantage is that all heat for DHW production has to be provided by the boiler.
- **HC V**. In order to avoid the disadvantage of the previous configuration, the cold domestic water is preheated by the principal heat producer using a heat exchanger. Given the high supply temperature of the CHP and its implications for the DHW tank (possibility of reversed heat transfer in the helical coil heat exchanger and destruction of stratification), this configuration is only considered for EHPs.
- **HC VI**. Rather than preheating the DHW tank's supply water with an extra heat exchanger, the coil heat exchanger can also be supplied by the principal heat producer directly. This concept is also applicable to cases with a CHP.

2.3. Simulations

All simulations can be performed with a simulation environment created in Matlab, partially developed in the context of the project 'Instal 2020' [41] which is, with exception of the DHW tank's internal heat exchanger, discribed previously [39, 42, 38]. The environment verifies energy balances at component level and at system level at all time steps, thereby ensuring correct programming of the simulation scripts. Only some aspects of the models that are required to interpret the results of the case studies are given. For detailed descriptions regarding the considered component models, the reader is referred to the latter cited work.

First of all, the behaviour of the inhabitants, i.e. settings of the set-point temperatures of the zones and usage of domestic hot water (DHW) was emulated by a 'statistical profile generator', which has been developed in previous projects [43, 41].

The models of the distribution system and building were implemented as following:

- Each individual apartment is represented as a single zone and described by a *2R2C* model [38]. The outdoor temperature and the solar heat gains throughout the year are defined by a Test Reference Year of Meteonorm based on meteorological data from Uccle, Belgium [44].
- The thermal behaviour of the emitters are represented by a dynamic radiator model with three uniform segments [45, 46]. The outgoing temperature at steady state is estimated maximum 2.9°C too high [38], compared to an LMTD (Logarithmic Mean Temperature Difference [47]) model.
- A plug-flow pipe model analogue to type 31 in TRNSYS Library[48] was implemented [49].
- A stratified thermal storage tank model analogue to type 4 in TRNSYS Library [48] is considered. For the DHW tank, a term to take heating from the internal heat exchanger is included. The corresponding equations are given in the appendix, in which also the protocol is given to enable fast calculations of this heat exchange: vectorised instead of sequential calculations for the different segments.

The thermal model of all three heat production components (CHP, EHP and boiler), is given by the following equation:

$$C_{prod}\,\frac{\mathrm{d}T_{out}}{\mathrm{d}t} = \dot{Q}_{th} - UA_{loss,skin}\,(T_{out} - T_{env}) - \dot{Q}_{hyd} \tag{1}$$

with: T_{out} (K) the temperature of the thermal mass of the producer, C_{prod} $(J\,K^{-1})$ the overall thermal capacity of the producer, $\dot{Q}_{th}$ (W) the heat transfer between the heat source and the thermal mass, T_{env} (K) the temperature of the surroundings of the envelope and $UA_{loss,skin}$ $(W\,K^{-1})$ the overall heat transfer coefficient of the envelope. $UA_{loss,skin}$ was fitted on catalogue data based on the skin losses at nominal conditions. $\dot{Q}_{hyd}$ (W) is the heat transfer towards the hydronic system, equal to $\dot{Q}_{hyd} = c\,\dot{m}\,(T_{out} - T_{in})$, with c $(J\,kg^{-1}\,K^{-1})$ the specific heat capacity of water, T_{in} (K) the inlet water temperature and $\dot{m}$ (kg/s) the mass flow rate of the water.

In the context of building system simulations, Equation 1 is a typical one to describe the dynamics of boilers [50, 51, 52, 53] and it was also applied on ICE-CHPs [54]. To obtain consistency in model structure for all three heat producers, a minor adjustment of the heat pump model used by others [55, 56, 57] was made. Indeed, instead of applying a first order delay on the heat transfer within the condenser to include dynamic behaviour, here this delay is applied on the temperature of the condenser.

For the CHP and boiler, $\dot{Q}_{th}$ is assumed to be controlled directly by internal control logics, while for the EHP it is considered to be the result of its source and sink temperatures (quantified by a second order polynomial [39]). For the CHP, $\dot{Q}_{th}$ is at its nominal value if the inlet temperature is below 70°C and decreases linearly to 50% between 70°C and 75°C. The CHP shuts down at an inlet or outlet temperature higher than 75°C and 90°C; the EHP at an inlet or outlet temperature above 55°C and 60°C, respectively.

The relation between thermal behaviour and the consumed energy (gas for the boiler or CHP and electricity for the EHP) is given by a so called *performance map.* The boiler's performance map is given by an instantaneous thermal efficiency as a generalised function of inlet temperature, outlet temperature and part load ratio [58, 59]. It includes the non-linear effect of temperature levels on condensation gains and the effectiveness of the combustion heat exchanger. The performance map of the heat pump is, again, given by a second order polynomial in function of its source and sink temperatures [39]. Finally, the CHP's performance map takes a linear effect of the inlet temperature and part load into account. Also its electrical efficiency is approximated by a linear function, but only in function of the part load ratio [38].

The hydraulic models of control valves and pumps are simplified in order to reduce model complexity and decrease computation time. This means that control signals are considered to affect flow rates directly, without relying on models based on fluid mechanics. The assumptions and implications of this simplification has been discussed in previous work [38].

In what follows, the simulations performed in this step are referred to as the 'main simulations'. This allows to distinguish them from the reference simulations that are used to generate the Demand Load Profile and Production Load Profile.

2.4. Analysis and selection

In this paper, 'extended Load Duration Curves' are proposed as a comprehensible measure for evaluating hydronic configurations. They allow to evaluate a configuration on a single graph, while still providing some explanation of its behaviour. It should give the designer an idea about the overall performance, and allow to detect faults and benefits without necessarily looking into the large amount of simulation data from the previous step.

To explain the basic idea behind the extended LDCs, an example is given in Figure 3. The three colors represent three components of the production system: boiler (red), principal heat producer (green) and tank (blue). As is the case for conventional LDCs, the figure shows the total heat load in descending order. The extended LDC, however, adds information by providing insight in how this heat is delivered by the production system:

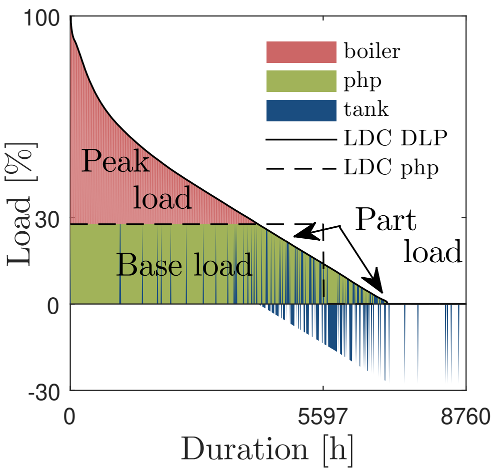

Figure 3: An example of an extended Load Duration Curve (LDC), with the three differently coloured areas referring to different components of the production system (php stands for principal heat producer). Also the LDC of the principal heat producer is shown and reveals the yearly operational hours.

- The LDC of the principal heat producer itself is shown as a dotted line. It shows its total operating hours (were the line collides with the x-axis, for this example equal to 5597h) and its total amount of produced heat (area under the line). Note that the tank enables the principal heat producer to operate also at low loads, thereby extending the total operation time.
- The upper area, denoted by the term 'Peak load', represents the heat delivered at loads higher than what the principal heat producer can generate, typically a situation in which the boiler provides back-up heat.
- The principal heat producer covers the 'Base load', which is shown as an area that is limited by the producer's nominal thermal load. This nominal load is shown on the y-axis and is in this example equal to 30% of the building full load.
- From the principal heat producer's point of view, the building is in 'Part load' if the demand is lower than the formers nominal load. As a result, this area represents two typical situations: the principal heat producer is ON and the excess heat is stored in the tank (blue area's below x-axis) or it is OFF and the heat is delivered by the tank (blue area's above x-axis).
- The solid black line shows the LDC of the Demand Load Profile (DLP). In this example, the demand load matches the production load exactly.

According to the present methodology, these extended load duration curves are generated for both the Production Load Profile (PLP). The LDC of the PLP is intended to show the designer the behaviour of the production system, as expected based on thermal loads only. The LDCs based on the main simulations reflect the behaviour of the production system including the effect of the hydronic configuration. Showing both allows the user to distinguish the effect of the production-specific boundary conditions from the actual effect of the hydronic configuration. Given the common use of conventional LDCs, it is expected that the proposed extended LDCs are easily accessible for all stakeholders in design processes.

Besides this qualitative analysis, also a quantitative evaluation is possible for all the hydronic configurations. First, to describe the effect of an hydronic configuration on the demand side performance, the following Key Performance Indicators (KPI's) are used:

- p_{Qsh}^{ref}: the extra building's thermal energy consumption that is used to heat the building, relative to the value corresponding to the DLP (in %). The building's thermal energy consumption is defined as the total thermal energy transferred from the production system to the end use by the distribution system.
- p_{Qdhw}^{ref}: the extra building's thermal energy consumption that is used to deliver DHW to the end users, relative to the value corresponding to the DLP (in %).
- The Room Temperature Lack (RTL) and Sanitary Temperature Lack (STL) quantify the discomfort of the space heating and domestic hot water as experienced by the end users, respectively. These variables are expressed in number of degree hours per day, and a Temperature Lack (TL) within a period $t_2 - t_1$ is, in general, calculated as follows [52]:

$$TL = \int_{t_1}^{t_2} (T_{sp} - T_{pv})\,\mathrm{d}t \quad \text{if } T_{pv} < T_{sp} \tag{2}$$

  With T_{sp} the set point temperature and T_{pv} the process value. r_{rtl}^{ref} and r_{stl}^{ref} are, respectively, defined as the ratio of RTL and STL of a particular hydronic configuration to the RTL and STL of the corresponding the DLP.

The effect of the hydronic configuration on the performance of the production system and its components, is given by the following KPIs:

- η_{yea}: the CHP is evaluated by its yearly electrical ($\eta_{el,yea}^{chp}$) and thermal ($\eta_{th,yea}^{chp}$) efficiency, and the boiler by its yearly thermal efficiency (η_{yea}^{boi}). For consistency of notation, the yearly Seasonal Performance Factor of the EHP is referred to as η_{yea}^{ehp}. These yearly thermal efficiencies are defined as the total heat transferred from a producer to the heating system, over the total energy usage (gas for boiler and CHP, electricity for the heat pump), and analogue for the yearly electrical efficiency of the CHP.
- t_{cyc}: the mean continuous operation time in hours between a start-up and shut-down of the principal heat producer (t_{cyc}^{chp} and t_{cyc}^{EHP}) and boiler (t_{cyc}^{boi}). It quantifies the stability of operation: the higher the value the less maintenance costs can be expected. The advantage of this variable over e.g. the total number of start-ups is that it takes into account the total operation time.
- q_{php}^{tot}: the share of heat produced by the principal heater. $100 - q_{php}^{tot}$ is, obviously, produced by the boiler.
- $RPES$: the relative primary energy savings are calculated with a reference electrical and thermal efficiency of 37% and 90% (based on higher heating value), respectively, that represent the best available conventional heat and electricity production alternative, as discussed by Verhaert et al. [60]. This variable takes both the principal heat producer's and boiler's performance into account.

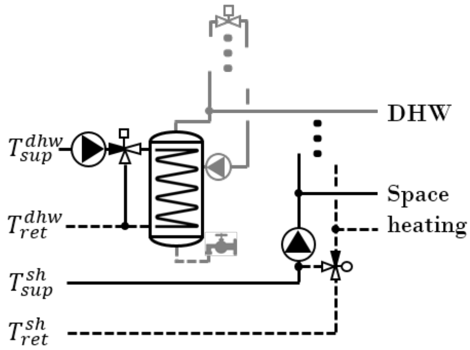

Figure 4: The heat distribution system for space heating and DHW. Connections to the central pipes of only a single apartment unit are shown; the other connections are represented by the ellipses. See Figure 2 for a legend of the symbols.

3. Case studies: applying the design methodology

This section illustrates the present design methodology for a variety of case studies and, based on that, formulates general guidelines that can assist future design processes. As already mentioned, it should be noted that this paper does not aim to compare the different boundary conditions as such.

In the first subsection, the considered demand- and production-specific boundary conditions of all case studies are discussed. To facilitate the illustration of the methodology, it is decoupled from the overall design process of a building by generating the DLP (Demand Load Profile) and PLP (Production Load Profile) by reference simulations, rather than obtaining them by a real design process.

The results of the case studies are addressed in the subsection thereafter. Finally, this section concludes with a general discussion regarding the proposed methodology and guidelines for future projects.

3.1. Case descriptions

3.1.1. Demand-specific boundary conditions

All case studies are based on an apartment building consisting of 24 identical apartment units, with exception of their solar orientation. The behaviour of inhabitants is represented by both comfort demands and DHW usage. More specifically, the types of the different families living in the 24 apartment units match a typical distribution of Flemish families [61], as was determined in previous projects [43, 41]. A separate distribution circuit is considered for space heating and DHW, as can be seen in the Distribution BCs of Figure 2 and, in more detail, in Figure 4.

The water in the common DHW pipe is not allowed to cool down below 60 °C during periods of inactivity, in order to prevent long waiting times for DHW users and to avoid risk of *Legionella* growth [62]. Therefore, a control valve allows circulation if the water temperature drops below the limit (Figure 4). The DHW is stored in the DHW tank, which is kept at 70 °C by an internal helical coil heat exchanger. The corresponding pump goes ON if the temperature decreases below its set-point. To prevent reversed heat transfer across the coil, i.e. when the outlet temperature T_{ret}^{dhw} becomes higher than the inlet temperature T_{sup}^{dhw}, a three-way valve bypasses the supply water if its temperature, T_{sup}^{dhw}, is too low to heat the DHW tank.

Two different sizes of helical coil heat exchanger of the DHW tank are considered: one corresponding to, respectively, an inlet ($T_{sup,des}^{dhw}$) and outlet ($T_{ret,des}^{dhw}$) design temperature of 75°C and 65°C, and one of 75°C and 35°C (see Figure 4).

The size of the DHW tank is based on a methodology developed by Verhaert et al. [63] which limits the required peak demand of the production system. The sizing, that takes heat losses and temperature sensor positions into account, resulted in a total tank volume of $114l$. Regarding the sensors, it should be mentioned that the upper sensor is positioned at 50% of the tank height. This ensures that the upper half of the tank is able to cover for peak demands in DHW.

The design heat loss of each apartment unit is 5 kW at 22 °C indoor and -8 °C outdoor temperatures. Two different types of heat emitter are considered: radiators and underfloor heating. Radiators are sized with inlet ($T^{sh}_{sup,des}$) and outlet ($T^{sh}_{ret,des}$) design temperatures of 75°C and 65°C and underfloor heating systems with 45°C and 35°C, respectively. Weather compensation is applied on the supply temperature set-point for space heating.

The room temperature set-point during non-sleeping occupancy of an apartment unit is 22 °C. During sleeping or absence, a lower set-point is considered, equal to 15 °C for cases with radiators and to 20 °C for cases with underfloor heating. The higher value for cases with underfloor heating take into account slower thermal response. All these considered temperature levels, as well as these of the DHW system are summarised in Table 1.

Table 1: Summary of the considered demand-side variations. Different temperature levels for both space heating and DHW production are considered. For the lower and higher temperature regime for space heating, underfloor heating and radiators are considered as emitter, respectively.

Case	$T^{sh}_{sup,des}/T^{sh}_{ret,des}$ °C	$T^{dhw}_{sup,des}/T^{dhw}_{ret,des}$ °C	Q_{sh} $[10^{12}J]$	Q_{dhw} $[10^{11}J]$	RTL $[Kh/day]$	STL $[10^{-3}Kh/day]$
A	75/60	75/60	1.03	1.6	14.38	0.79
B	45/35	75/60	1.35	1.6	10	0.95
C	75/60	75/35	1.03	1.6	14.4	1.1
D	45/35	75/35	1.35	1.6	10	1.2

The DLP is generated by the same simulations as used for the evaluation of the hydronic configurations, but with the hybrid heat production system replaced by an idealised boiler. This allows to quantify the behaviour inherent to the demand-side specific boundary conditions, which is used as a reference in the analysis and selection step of the design. Besides generating the DLP, the reference simulation reveals the total consumed heat for space heating and DHW production for case A, B, C and D, and corresponding RTL and STL (given in Table 1).

While a detailed comparison between the cases themselves is outside the scope of this paper, the results are explained briefly. The higher consumption for space heating of case B and D are explained by the higher set-point temperatures during absence or inactivity if underfloor heating is considered as boundary condition. This can also explain the slightly lower RTL for these cases, as a lower temperature increase is required if the set point changes from its lower to its upper value. For case A and C, DHW is responsible for 13% of the final thermal energy consumption, and 11% for case C and D. The space heating-related discomfort (expressed in Room Temperature Lack) can be interpreted as follows: for all cases, spoken in terms of mean values, the temperature is between 10 and 15 hours one degree Celsius below its set-point in a day. The Sanitary Temperature Lack is negligible; in other words, a high enough supply temperature, T^{sh}_{sup}, is provided by the distribution system for all cases.

3.1.2. Production-specific boundary conditions

To make abstraction of the numerous existing optimisation algorithm for technology selection, sizing and control strategy, choices are made based on rules of thumb, as often used by design engineers. It is therefore assumed that the design process preceding the present methodology results in the following boundary conditions:

- **Technology selection**. For all cases (A to D), a boiler is selected as auxiliary heater. As principal heat producer, either a CHP or an EHP is selected. In what follows, these different boundary conditions are treated as different cases: cases 'CHP-A' to 'CHP-D' and cases 'EHP-A' to 'EHP-D'.

- **Sizing**. The principal heat producer is sized to cover 30% of the total load required at design conditions (120kW), hence a 36kW nominal thermal load is considered.

  The boiler is sized to match the full 120 kW; this ensures comfort at OFF-time of the principal heat producer. For an EHP shut-downs are likely to occur when operated at too high temperatures and for

Table 2: Overview of the considered case studies and hydronic configurations. 'A', 'B', 'C' and 'D' refer to demand-specific boundary conditions as given in Table 1

Producer	Case	Configurations
CHP	CHP-A	HC I, IIo/c, IImod, III, IV, VI
	CHP-B	HC I, IIo/c, IImod, III, IV, VI
	CHP-C	HC I, IIo/c, IImod, III, IV, VI
	CHP-D	HC I, IIo/c, IImod, III, IV, VI
EHP	EHP-A	HC I, IIo/c, IImod, IV, V, VI
	EHP-B	HC I, IIo/c, IImod, IV, V, VI
	EHP-C	HC I, IIo/c, IImod, IV, V, VI
	EHP-D	HC I, IIo/c, IImod, IV, V, VI

a CHP a maximum number of ON/OFF cycles may also disable its operation temporarily. Besides, for both types of heat producers, maintenance can restrict operation.

A thermal storage tank is sized to guarantee a minimal operating time of one hour for the principal producer.

- **Control strategy**. The principal heat producer is controlled based on the thermal demand, which is reflected in the state of charge of the tank. The auxiliary heater provides back-up if the produced heat by the principal heater is not sufficient.

Based on these boundary-conditions, the Production Load Profile (PLP) is generated by a reference simulation, based on only heat flows (as typical optimisation algorithms do):

- The Demand Load Profile (DLP) is taken as input and at all time, the total thermal demand load is covered by the production system.
- If a CHP is considered as principal heat producer, it is characterised by a constant thermal energy production if it is ON.
- Also for the EHPs a constant thermal output is considered, but it is limited depending on the temperatures defined by the DLP.
- A storage tank is described by a maximum energy content only, i.e. regardless of the temperature of the water it contains.
- The boiler provides the extra heat that is required to fulfil the thermal demand load defined by the DLP.

The resulting PLP sets a reference regarding the behaviour of the production system, regardless of the hydronic configuration.

All the case studies that are considered are summarised in Table 2; in total, 48 full year simulations were performed.

3.2. Results and discussion

In this subsection, first the effect of the hydronic configurations on the demand-side performance is discussed for all cases. Then, the production-side performance is analysed for all cases with a CHP as principal heat producer and after that, for those with an EHP.

3.2.1. Demand-side performance

For all cases, all hydronic configurations result in thermal energy consumption of the building and discomfort experienced by its inhabitants (in terms of Room Temperature Lack and Sanitary Temperature Lack) close to the DLP simulation. The total thermal energy consumption differs less than ±1% for both space heating (p^{ref}_{Qsh}) and DHW production (p^{ref}_{Qdhw}). The RTL is always less than 1.1 times the reference (r^{ref}_{rtl}) and the discomfort experienced by DHW consumers is always less than the double of the reference (r^{ref}_{stl}). Given the low values of STL of the DLP ($10^-3Kh/day$, see Table 1, even values twice as high are acceptable. In conclusion, all hydronic configurations result in a demand-side performance close to what is inherent to the demand-specific boundary condition. Therefore, the rest of the discussion focusses on the production-side performance.

3.2.2. Production-side performance for cases with Combined Heat and Power (CHP)

In what follows, first the extended Load Duration Curves (LDCs) are discussed in order to illustrate their usability, and after that the performance of all configurations is examined.

Figure 5 shows the extended LDCs of both the Production Load Profile (PLP) and all six hydronic configurations for cases CHP-A to CHP-D. While the behaviour of the production system shows clear similarities between the expected behaviour (PLP) and the different configurations (main simulations) for all four cases, none behaves exactly as expected. Two major types of deviation and their interpretation are explained hereafter.

First, the CHP LDCs show that the CHP operates more hours than expected: depending on the configuration between 5983 and 6368 hours instead of 5619 hours. This is because if a net flow from bottom to top occurs in the tank it can -temporarily- cover net extra load on top of what the CHP is producing. For all six configurations, this can be seen in Figure 5: a part of the 'base load' (and even 'peak load') is covered by the tank (blue), for which a part of the 'peak load' can be covered by the CHP.

Second, the tank is not only charged by the excess heat of the CHP under 'part load' conditions but also at higher thermal demand. This is especially true for HC I, HC III and HC VI. It makes no sense to store heat from the CHP if the heat demand of the building is higher than what the CHP can produce. Two causes of this unexpected behaviour are discussed.

The first cause is a high return temperature that can charge the tank, as shown for configurations HC I, HC IIo/c and HC IImod in Figure 6. The first row of plots shows the temperature in the DHW tank, and the second the return temperature (blue) and the temperature in the tank. The third displays the mass flow rate at the sink (black) and source (green) side of the tank, and the difference between the two (net through tank, negative if flow from bottom to top). The charging of the DHW tank starts at 55.1 h and, accordingly, the temperature of the DHW tank increases. A similar charging of this DHW tank can be observed for the three hydronic configurations. With increasing DHW tank temperature, also the return temperature increases for all configurations, during the shown example from more or less 35 °C up to 65 °C (second row of plots). For HC I, all the return water flows towards the tank, while for the two HC II concepts, a part of it flows towards the boiler (see Figure 2). For HC I this results in a high net flow rate from bottom to top (blue), as the source side flow rate (green) is considerably lower than sink side (black). As a result, the tank is being charged by the return water. While the HC IIo/c can partially solve this problem, HC IImod is almost able to eliminate it, i.e. to reduce the net tank flow to close to zero. While HC III and HC VI are characterised by the same flow towards the tank as HC I, HC IV is not affected by the charging of the DHW tank.

The second cause is a typical disadvantage of HC IIo/c as already before in detail examined [37, 38]. The parallel flow towards the boiler results in a net flow in the tank from top to bottom. As a consequence, the CHP charges the tank until a shut-down, even if the building requires more heat than the CHP is producing. This is an extra aspect that explains the improved tank flow balance of HC IImod compared to HC IIo/c.

Hereafter, the Key Performance Indicators are discussed in order to evaluate the hydronic configurations quantitatively.

First of all, it is mentioned that, regardless of the demand-specific boundary conditions, the hydronic configuration hardly affects CHP thermal efficiency,$\eta^{chp}_{th,yea}$ and electrical efficiency $\eta^{chp}_{el,yea}$ they vary for all

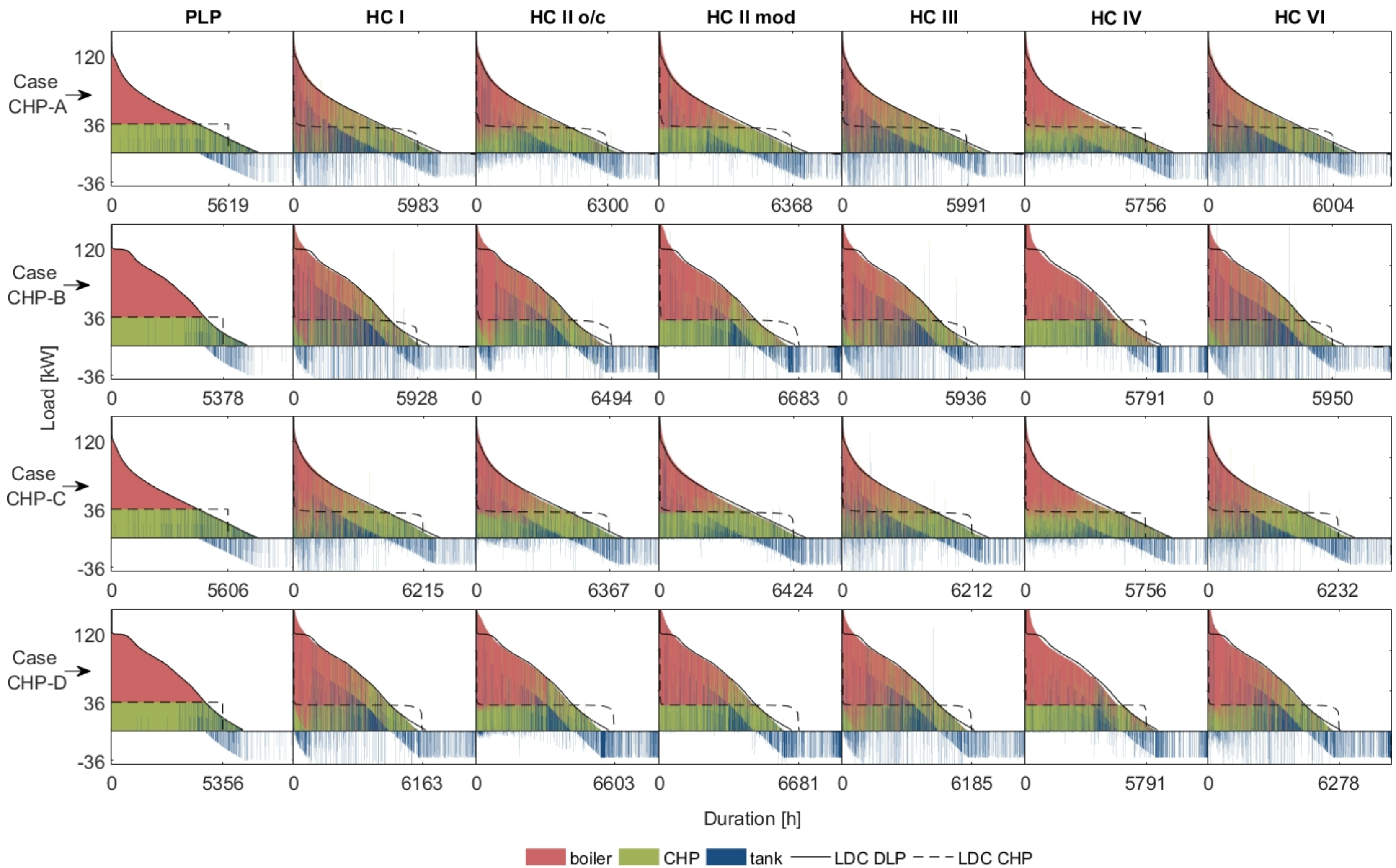

Figure 5: Extended Load Duration Curves for cases CHP-A, CHP-B, CHP-C and CHP-D.

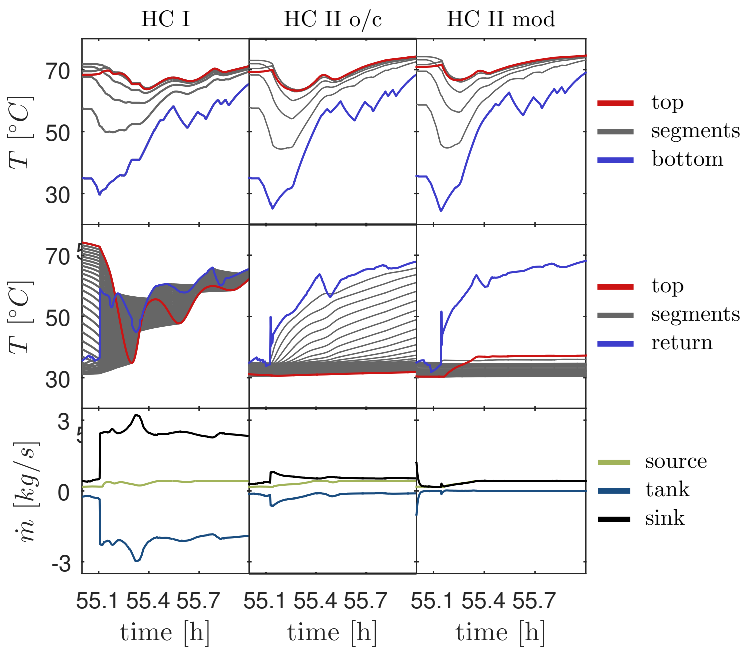

Figure 6: Dynamic data of one hour for case CHP-A to show the charging of the tank caused by a high return temperature. Meaning of the legend items: 'top' = the upper finite volume of tank or DHW tank, 'segments' = the different finite volumes, 'bottom' = the lower finite volume of tank or DHW tank, 'return' = return water, 'source' = at source side of tank, 'tank' = flow rate in tank itself (negative if flow from bottom to top) and 'sink' = at sink side of tank. Time is given in hours since January the first at midnight.

cases and hydronic configurations only between 62.1% and 62.9%, and 25.6% and 26.0%, respectively. Also the boiler performance shows only little variation, both in terms of efficiency, η^{boi}_{yea} (less than two percentage point difference) and mean continuous operating time, t^{boi}_{cyc} (less than 0.7h difference).

The stability of operation of the CHP is substantially affected by the hydronic configuration, though: t^{chp}_{cyc} is for HC IV more than three times higher than the other configurations (see Table 3). This can be explained by the absence of high return temperatures during DHW tank, as discussed above.

Table 3 reveals that also the performance at system level is affected by the hydronic configuration. Indeed, the share of heat produced by the CHP, q^{chp}_{yea}, is systematically the highest for HC IImod, followed by HC IIo/c.

Given the negligible differences in $\eta^{chp}_{th,yea}$, $\eta^{chp}_{el,yea}$ and η^{boi}_{yea}, q^{chp}_{yea} can be seen as the principal influence on the Relative Primary Energy Savings, $RPES$ and, as a consequence, HC IImod yields the best results. Besides $RPES$ itself, also the relative difference with HC I, $\Delta RPES$, is given by Table 3. The results reveal that, depending on the case, HC IImod achieves between 10.9% and 43.7% higher $RPES$ than HC I.

In conclusion, HC IImod should be selected, regardless of the emitter or heating coil temperature design levels.

3.2.3. Production-side performance for cases with an Electrical ground-coupled Heat Pump (EHP)

Also EHPs charge the tank at high demands, and not only at 'part load' condition, as shown by the extended LDCs (Figure 7). However, in contrast to CHPs, this behaviour is expected because at a supply temperature set point higher than what the EHP can provide, boiler operation is required. This can result in excess heat of the EHP, even at high thermal demand: it is inherent to the boundary conditions of the design and cannot be solved completely by optimising the hydronic configuration, as evidenced by the extended LDC of the Production Load Profile (PLP).

Nonetheless, if a separate circuit for the heating of the DHW tank is considered, this behaviour can be limited. Indeed, HC IV and HC V show substantially less tank charging at high demands. Since a fully

Table 3: Key Performance Indicators for all hydronic configurations and all case studies.

Case	KPI	Hydronic Configuration						
		I	IIo/c	IImod	III	IV	V	VI
CHP-A	t_{cyc}^{chp} [h]	7.0	6.3	6.3	6.5	23.1		7.0
	q_{yea}^{chp} [%]	56.8	59.8	60.6	56.8	56.4		57.1
	$RPES$ [%]	16.1	19.3	19.8	16.3	16.2		16.4
	$\Delta RPES$ [%]	0 (ref)	19.3	22.9	1.3	0.6		1.6
CHP-B	t_{cyc}^{chp} [h]	7.9	5.9	6.3	7.8	29.0		8.0
	q_{yea}^{chp} [%]	44.2	48.4	49.9	44.2	44.7		44.4
	$RPES$ [%]	14.1	18.5	20.3	14.4	15.7		14.4
	$\Delta RPES$ [%]	0 (ref)	31.2	43.7	1.6	10.8		1.6
CHP-C	t_{cyc}^{chp} [h]	11.4	11.8	12.4	11.6	23.1		11.6
	q_{yea}^{chp} [%]	60.3	61.9	62.5	60.3	56.4		60.5
	$RPES$ [%]	19.8	21.6	21.9	20.2	16.3		20.0
	$\Delta RPES$ [%]	0 (ref)	9.0	10.9	2.3	-17.7		1.2
CHP-D	t_{cyc}^{chp} [h]	11.7	12.8	12.1	11.4	28.8		11.8
	q_{yea}^{chp} [%]	47.1	50.5	51.1	47.3	44.7		48.0
	$RPES$ [%]	17.8	21.4	22.0	18.4	15.8		19.0
	$\Delta RPES$ [%]	0 (ref)	20.2	23.4	3.2	-11.2		6.3
EHP-A	t_{cyc}^{ehp} [h]	1.1	0.4	1.2		2.1	2.3	1.0
	q_{yea}^{ehp} [%]	38.8	27.2	41.2		52.4	55.2	37.5
	$RPES$ [%]	16.5	11.3	17.2		23.5	25.6	15.8
	$\Delta RPES$ [%]	0 (ref)	-31.6	4.2		42.1	54.8	-4.2
EHP-B	t_{cyc}^{ehp} [h]	2.3	1.4	4.0		10.2	9.4	2.7
	q_{yea}^{ehp} [%]	24.2	19.1	30.6		42.3	43.7	22.7
	$RPES$ [%]	15.5	12.8	19.3		27.8	28.9	14.6
	$\Delta RPES$ [%]	0 (ref)	-17.3	24.3		79.1	86.8	-5.6
EHP-C	t_{cyc}^{ehp} [h]	1.1	0.4	1.2		2.1	2.3	1.3
	q_{yea}^{ehp} [%]	42.7	28.2	42.6		52.4	55.3	43.9
	$RPES$ [%]	18.4	11.8	17.8		23.6	25.6	18.9
	$\Delta RPES$ [%]	0 (ref)	-35.7	-3.0		28.4	39.7	2.7
EHP-D	t_{cyc}^{ehp} [h]	3.6	1.3	4.2		10.5	9.6	4.2
	q_{yea}^{ehp} [%]	31.8	19.7	31.6		42.4	43.7	32.9
	$RPES$ [%]	20.1	13.4	20.4		28.1	29.2	21.7
	$\Delta RPES$ [%]	0 (ref)	-33.4	1.5		39.8	45.1	7.8

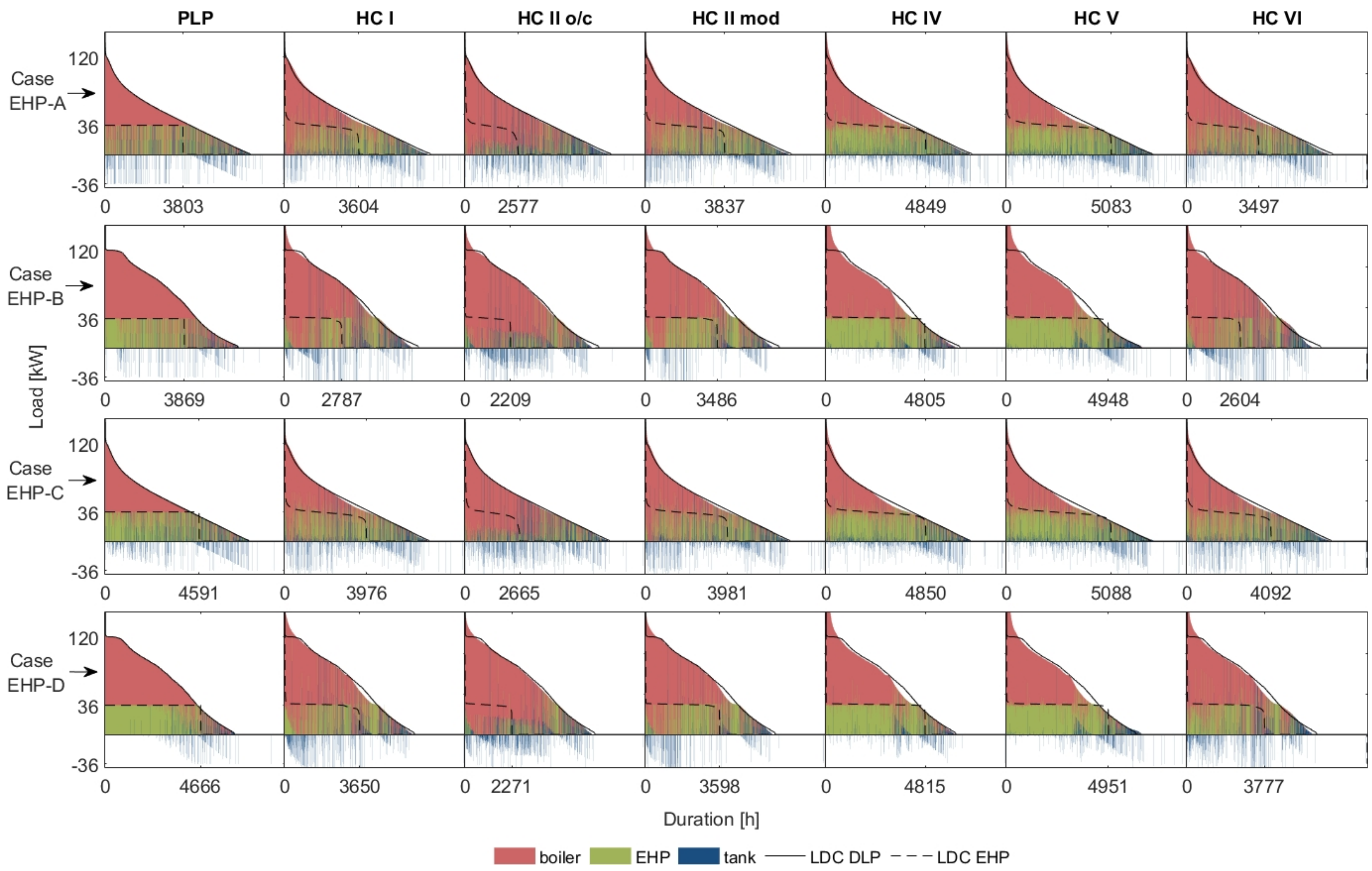

Figure 7: Extended Load Duration Curves for cases EHP-A, EHP-B, EHP-C and EHP-D.

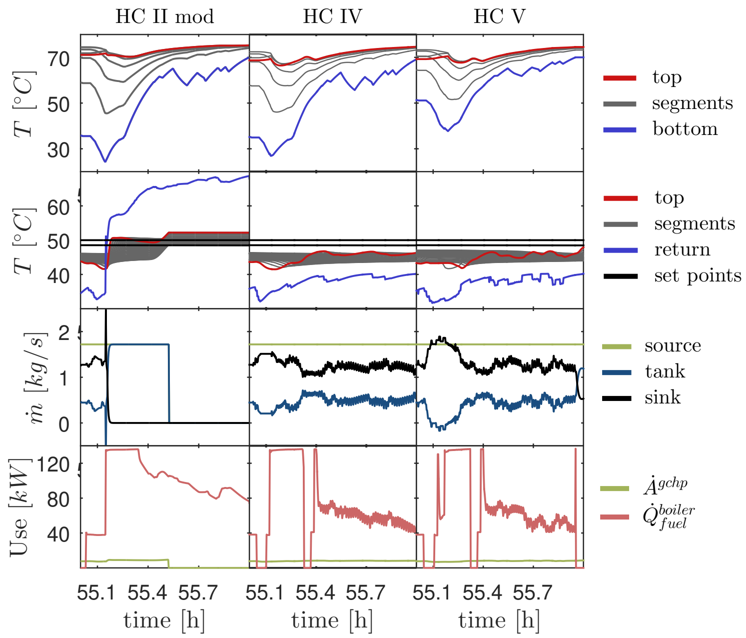

Figure 8: Dynamic data of one hour for case EHP-A to show the behaviour during DHW tank charging. Meaning of the legend items: 'top', 'segments', 'bottom', 'return', 'source', 'tank' and 'sink' as in Figure 6; upper and lower line of 'set points', respectively, bypass threshold of three-way valve of tank (50°C) and shut-down threshold for EHP (determined by weather compensation curve, in this example 48 °C), '$\dot{A}^{EHP}$' = EHP electricity uptake and '$\dot{Q}^{boiler}_{fuel}$' = fuel uptake of boiler. Time is given in hours since January the first at midnight.

charged tank shuts down the EHP, this also explains the highest operating time of HC IV and HC V: $4849h$ and $5083h$, respectively. The other configurations are clearly disadvantaged by the mixing of the circuits for space heating and DHW tank charging, e.g. HC IIo/c and HC IImod have an operation of only $2577h$ and $3837h$, respectively.

For HC IImod, HC VI and HC V, an example of dynamic data is shown by Figure 8. The upper plots show that a charging cycle of the DHW tank starts at $55.1h$. With charging of the DHW tank, the return temperature increases suddenly under HC IImod (second row of plots). As of the moment that this return temperature reaches the threshold of the tank three-way valve (upper black line in second row of plots, equal to 50°C), that water is bypassed. As a consequence, the flow rate at the sink side of the tank decreases to zero (third row, black line). Because the EHP stays ON (green line in fourth row) the tank is charged rapidly, and when its temperature at the bottom increases above its set point (in this example 48°C as determined by the weather compensation curve) the EHP shuts down. In contrast, for HC IV and HC V neither the threshold for bypassing the return water nor the threshold of the EHP are reached, thus no shut down occurs.

Upper behaviour is reflected in the yearly performance, shown in Table 3. Considering case EHP-A, HC IV and HC V show the highest share of heat produced by the EHP, q^{ehp}_{yea}, of 52.4% and 55.2% which also yields the highest $RPES$ of 23.5% and 25.6%, respectively.

An extra advantage of HC IV and HC V is the more stable operation of the EHP, quantified by t^{ehp}_{cyc}, which is almost twice that of the other configurations. As for the cases with a CHP, other KPIs vary only little for the different configurations (η^{ehp}_{yea}, $\eta^{boi}_{yea}$and t^{boi}_{cyc}).

The exact same trends can be seen for cases EHP-B to EHP-D: the highest operation time is consistently achieved with HC V, and so is the highest q^{ehp}_{yea} and $RPES$. Depending on the case, HC V scores 39.7% to 86.8% higher than HC I (see $\Delta RPES$ in Table 3). While HC VI comes close ($\Delta RPES$ varies between 28.4% and 79.1%), the difference with the other configurations is substantially ($\Delta RPES$ up to -35.7%).

These results encourage the selection of HC V, no matter which emitter or heating coil temperature design levels are considered.

3.3. General discussion

For all cases with a CHP as principal heat producer, HC IImod was found the best solution in terms of $RPES$. For all cases with an EHP, HC V is to be preferred based on the same KPI. The choice of hydronic configuration is hence sensitive towards the production-specific boundary conditions, more specifically the technology used as principal heat producer. In contrast, the sensitivity analysis on the demand-specific boundary conditions revealed that the decision of configuration is independent of the design temperature levels. Based on these findings, the following general guidelines are formulated for cases with distribution and emitter systems as considered in the present paper:

- If a CHP serves as principal heat producer, the hydronic configuration should be chosen to prevent improper charging of the tank. Of all considered solutions, the optimal way to do this is by allowing a parallel flow towards the boiler and control that flow with a modulating valve.
- With an EHP as principal heater, the circuit for space heating and that for heating the DHW tank should be separated. Preheating of the DHW tank water content is preferred in order to allow the EHP to cover the DHW heat partially.

For cases EHP-B and EHP-D, for which DHW account for 11% of the heat demand, preheating increases q_{yea}^{ehp} with only $1.4p.p.$ and $1.3p.p.$ (Table 3). For cases EHP-A and EHP-C, which have a higher DHW demand of 13%, a higher advantage of preheating is observed: q_{yea}^{ehp} increases with 2.8% and 2.9%, respectively. Hence, it is expected that for buildings with a higher share of DHW heat demand, e.g. by a higher insulation level, the potential of preheating further increases.

By means of two examples, the authors stress that the two formulated guidelines cannot be generalised to any case, though. First, the DHW tank can also be heated by an external heat exchanger. The resulting improved stratification, compared to an internal heat exchanger, is expected to avoid the sudden increase of the return temperature during DHW tank charging. Second, other distribution systems exist to cover both DHW and space heating in collective systems. A frequently used concept is by using common pipes for the distribution of heat for both DHW and space heating. Heat Interface Units transfer this heat to either the space heating or DHW system at a local level [64], and therefore the production of DHW is spread out more in time. It is clear that for both examples the evaluation of all hydronic configurations should be remade.

The proposed methodology proved successful in selecting an hydronic configuration with the highest performance. Therefore it is expected that it is able to do the same for other cases, such as characterised by the two upper examples. Indeed, the steps of the methodology are verified by this research: setting up a morphological chart, performing the simulations, analysing the results for selecting the final hydronic configuration, and formulating guidelines. It should be mentioned, though, that a Graphical User Interface might facilitate the application of the methodology to other types of hybrid production systems than discussed in this work.

In particular the use of the proposed 'extended LDCs' proved to be successful for analysing the simulation results. It gives the user an idea about the advantages and disadvantages of each hydronic configuration, without the need for exploring the enormous amount of simulation data. Also, by comparing the LDCs of the hydronic configurations with these of the DLP and PLP, the behaviour inherent to the boundary conditions can be distinguished from the actual effect of the hydronic configuration. This increases the comprehensibility of the design process, especially given the wide-spread use of conventional LDCs.

Besides providing insight in the behaviour, these LDCs can also directly assist decision making based on $RPES$. Indeed, they present the total operating time of the principal heater (where LDC of principal heater collides with the x-axis, see Figure 5 and 7) and its share of thermal heat production (the percentage green area). These two variables prove to be valid predictors to find the configuration with maximal $RPES$ for all cases, as shown by Figure 9.

LDCs should also be able to reflect the level of discomfort, relative to the Demand Load Profile (expressed in r_{rtl}^{ref} and r_{stl}^{ref}). While this could not be verified in the present work because of the low discomfort, it is

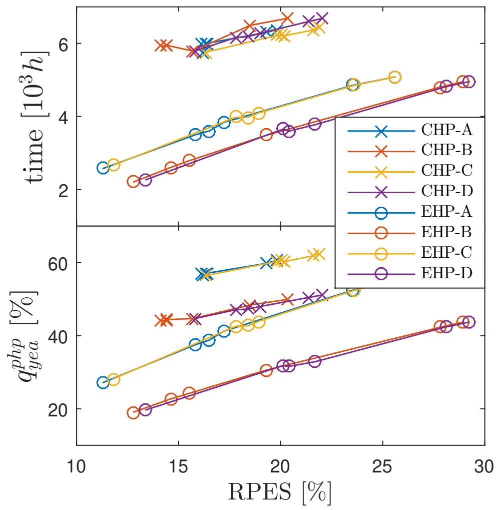

Figure 9: The potential of the total operating time and the share of heat produced by the principal heat producer to represent the RPES.

expected that for hydronic configurations which result in a higher discomfort than the Demand Load Profile (DLP), the LDC deviates from the DLP LDC. However, the LDCs are not able to provide information concerning the stability of operation and hence the use of it should be supported by a limited number of KPIs.

Finally, a note about the use of feedback of the analysis. Besides the formulation of generalised guidelines for future projects, as discussed above, another aspect can improve the overall design of heating systems within a particular project. Indeed, in future research the selection procedure of the hydronic configuration can be embedded in existing methodologies, such as discussed in the introduction. More specifically, the feedback can be coupled in order to develop a simulation-based optimisation method [65] that searches for optimal technologies, sizes, control strategies and hydronic configurations at once.

4. Concluding remarks

In this paper, a general methodology to design the hydronic configuration of hybrid heat production systems, consisting of a principal and an auxiliary heat producer, was presented. The methodology focusses on comprehensibility and consists of three steps: structuring possible solutions into a morphological chart, performing a simulation-based evaluation and selecting the best configuration based on a new type of Load Duration Curve (LDC).

The methodology was illustrated on eight case studies, all based on the same apartment building with a collective system with separate distribution pipes for both space heating and domestic hot water (DHW) production. The following production- and demand-specific boundary conditions characterising the case studies were considered: either an Internal Combustion Engine-based Combined Heat and Power device (ICE-CHP) or an Electric ground-coupled Heat Pump (EHP) as principal heat producer, underfloor heating or radiators as emitters and a large or a small coil heat exchanger to produce DHW. A condensing boiler was considered as auxiliary heater and to allow a stable operation of the principal heater, the latter was equipped with a storage tank. The following conclusions could be drawn:

- If an ICE-CHP is considered as principal heater, the boiler should be implemented in parallel to it and by using a modulating control valve. This ensures a qualitative management of the tank by, amongst others, preventing it from being loaded by a high return temperature during DHW production.

- For hybrid production systems with an EHP, the circuits of the production system for space heating and DHW should be separated. To allow the EHP to cover the DHW heat partially, preheating of the domestic cold water is recommended.

These findings are true, regardless of the emitter type or size of the heat exchanger to produce DHW. Selecting the correct hydronic configuration could increase the Relative Primary Energy Savings (RPES) with up to 6.2 percentage points for cases with a CHP, and for those with an EHP with up to 16.1 percentage points. It was found that maximising the operation of the principal heat producer leads to the highest RPES, rather than by optimising the performance of individual components.

In general, the proposed methodology proved to be successful in increasing the performance of hybrid heat production systems. The new type of LDC is able to provide information about the behaviour of each configuration in order to analyse its advantages and disadvantages, without the need for looking into the enormous amount of simulation data. It also allowed to select the configuration with the highest performance in terms of Relative Primary Energy Savings.

The authors acknowledge that the development of a morphological chart will remain a problem in design processes, though. Indeed, only limited and fragmented information is available on hydronic configuration. Therefore, we advocated the consistent use of the term 'hydronic configuration' to denote how components are connected by pipes, pumps and valves, and to develop a platform to centralise existing information on the topic.

In conclusion, the proposed methodology provides a comprehensible tool to assist the different stakeholders in their pursuit of high performance hybrid heat production systems. Future work should focus on the centralisation of information regarding the subject, through the development of an publically available platform.

Acknowledgements

We would like to express our sincere gratitude to *Hysopt*, *Viessmann*, *Remeha (BDR Thermea Group)*, *Continental Energy Systems (Lek/Habo Group)*, *Stiebel Eltron* and *Fixsus* for their valuable input regarding hydronic configurations.

Appendix

In this appendix, first the governing equations of the helical coil heat exchanger are given and, next, how these equations can be solved efficiently in order to limit computation time.

As discussed in the main text of this paper, the hot water storage tank itself is modelled according to type 4 in TRNSYS Library [48]. In this one-dimensional model, the tank is discretized into n finite volumes, each with a uniform temperature of its main water content T_i^{sto} with i ranging from 1 to n (from top to bottom). To add internal heating by the helical coil heat exchanger, the following assumptions are made:

- The thermal capacity of each finite volume is substantially larger than that of the piece of coil embedded in it. Based on that, the thermal inertia of the coil's metal is neglected. Also, the fluid in the coil is assumed to be at steady-state, given its relative fast dynamics.

- Also based on the relative high thermal inertia of the main water content, its temperature (T_i^{sto}) is considered constant during each simulation time step.

- The convective heat transfer between the two sides of the coil is substantially higher than diffusion within the coil; hence this latter type of heat transfer is neglected for the fluid in the coil.

For a single finite volume, with outlet and inlet temperature of the coil $T_{i,out}^{hea}$ and $T_{i-1,out}^{hea}$, respectively, the equations become:

$$T_{i,out}^{hea} = T_{i-1,out}^{hea} * e^{-NTU/n} + T_i^{sto}(1 - e^{-NTU/n}) \tag{3}$$

$$\dot{Q}_i^{hea} = -\dot{C}^{hea}(T_{i,out}^{hea} - T_{i-1,out}^{hea}) \tag{4}$$

with $\dot{Q}_i^{hea}$ (W) the heating of finite volume i, $NTU = \frac{UA^{hea}}{\dot{C}^{hea}}$ the Number of Transfer Units of the complete coil, and UA^{hea} (W/K) and $\dot{C}^{hea}$ (W/K) the overall heat transfer coefficient of the coil and the capacitive flow of the fluid in it, respectively. $T_{i-1,out}^{hea}$ for $i = 1$, $T_{0,out}^{hea}$, is the inlet temperature of the coil and is a known variable in what follows.

Since Eq. 3 is a recurrence relation, i.e. $T_{i,out}^{hea}$ depends on $T_{i-1,out}^{hea}$, direct calculations for all i are not possible. A possibility is to perform the calculations iteratively, i.e. calculating $T_{i,out}^{hea}$ subsequently for i is 1 to n. However, especially for simulations with high spatial resolution (high value for n), this is expected to increase the computation time substantially.

Therefore an alternative approach is proposed, which enables vectorised calculations of $T_{i,out}^{hea}$, i.e. for all i in once. The main idea of this approach is to calculate $T_{i,out}^{hea}$ by an explicit function of $T_{0,out}^{hea}$. To do so, the fictitious temperature $\bar{T}_{1,i}^{sto}$ is defined by the following equation:

$$T_{i,out}^{hea} = T_{0,out}^{hea} * e^{-i*NTU/n} + \bar{T}_{1,i}^{sto}(1 - e^{-i*NTU/n}) \tag{5}$$

$\bar{T}_{1,i}^{sto}$ can be interpreted as the mean of the temperatures T_i^{sto} for 1 to i weighted over the position along the flow direction so that the outlet temperature of the coil in the i-th segment can be calculated explicitly. To further interpret the meaning of $\bar{T}_{1,i}^{sto}$, the reader is advised to compare Equation 5 with Equation 3.

In what follows it is explained how the weights are defined, by deriving an expression for $\bar{T}_{1,i}^{sto}$.

First, Eq. 3 is written for $i = 1, 2, 3, i$:

$\underline{i = 1}$:

$$T_{1,out}^{hea} = T_{0,out}^{hea} * e^{-NTU/n} + T_1^{sto}(1 - e^{-NTU/n}) \tag{6}$$

$\underline{i = 2}$:

$$\begin{aligned} T_{2,out}^{hea} &= T_{1,out}^{hea} * e^{-NTU/n} + T_2^{sto}(1 - e^{-NTU/n}) \\ &= (T_{0,out}^{hea} * e^{-NTU/n} + T_1^{sto}(1 - e^{-NTU/n})) * e^{-NTU/n} + T_2^{sto}(1 - e^{-NTU/n}) \\ &= T_{0,out}^{hea} * e^{-2*NTU/n} + T_1^{sto}(1 - e^{-NTU/n}) * e^{-NTU/n} + T_2^{sto}(1 - e^{-NTU/n}) \end{aligned} \tag{7}$$

$\underline{i = 3}$:

$$\begin{aligned} T_{3,out}^{hea} &= T_{2,out}^{hea} * e^{-NTU/n} + T_3^{sto}(1 - e^{-NTU/n}) \\ &= (T_{0,out}^{hea} * e^{-2*NTU/n} + T_1^{sto}(1 - e^{-NTU/n}) * e^{-NTU/n} + T_2^{sto}(1 - e^{-NTU/n})) * e^{-NTU/n} \\ &+ T_3^{sto}(1 - e^{-NTU/n}) \\ &= T_{0,out}^{hea} * e^{-3*NTU/n} + T_1^{sto}(1 - e^{-NTU/n}) * e^{-2*NTU/n} + T_2^{sto}(1 - e^{-NTU/n}) * e^{-NTU/n} \\ &+ T_3^{sto}(1 - e^{-NTU/n}) \end{aligned} \tag{8}$$

$\underline{i = i}$:

$$\begin{aligned} T_{i,out}^{hea} = T_{0,out}^{hea} * e^{-i*NTU/n} &+ T_1^{sto}(1 - e^{-NTU/n}) * e^{-(i-1)*NTU/n} \\ &+ T_2^{sto}(1 - e^{-NTU/n}) * e^{-(i-2)*NTU/n} \\ &+ T_3^{sto}(1 - e^{-NTU/n}) * e^{-(i-3)*NTU/n} \\ &+ ... \\ &+ T_i^{sto}(1 - e^{-NTU/n}) * e^{-(i-i)*NTU/n} \end{aligned} \tag{9}$$

$T^{hea}_{out,i}$ can also be written as:

$$T^{hea}_{i,out} = T^{hea}_{0,out} * e^{-i*NTU/n} + (1 - e^{-NTU/n}) * \sum_{j=1}^{i} T^{sto}_{j} * e^{-(i-j)*NTU/n} \tag{10}$$

To find an analogy with Eq. 5, the second term of Eq. 10 is multiplied by $(1-e^{-i*NTU/n})/(1-e^{-i*NTU/n})$ and reorganised:

$$T^{hea}_{i,out} = T^{hea}_{0,out} * e^{-i*NTU/n} + \left(\frac{(1 - e^{-NTU/n})}{(1 - e^{-i*NTU/n})} * \sum_{j=1}^{i} T^{sto}_{j} * e^{-(i-j)*NTU/n} \right) * (1 - e^{-i*NTU/n}) \tag{11}$$

And hence $\bar{T}^{sto}_{1,i}$ in Eq. 5 is equal to:

$$\bar{T}^{sto}_{1,i} = \frac{(1 - e^{-NTU/n})}{(1 - e^{-i*NTU/n})} * \sum_{j=1}^{i} T^{sto}_{j} * e^{-(i-j)*NTU/n} \tag{12}$$

Finally, to calculate $T^{hea}_{i,out}$ for all i, Eq. 10 is written as:

$$T^{hea}_{i,out} = T^{hea}_{0,out} * e^{-i*NTU/n} + (1 - e^{-NTU/n}) * e^{-i*NTU/n} * \sum_{j=1}^{i} T^{sto}_{j} * e^{j*NTU/n} \tag{13}$$

In Matlab, Equation 13 can be calculated by elementary-wise operations on a vector $i = 1 : n$, and by using a cumulative sum for the summation operator in the right term. With the resulting outcome, Equation 4 can then finally be calculated -also vectorised.

References

[1] European Commission, https://ec.europa.eu/clima/policies/strategies.

[2] J. A. Moya, Impact of support schemes and barriers in Europe on the evolution of cogeneration, Energy Policy 60 (2013) 345–355. doi:10.1016/J.ENPOL.2013.05.048.
URL `https://www.sciencedirect.com/science/article/pii/S0301421513003844`

[3] J. Zimny, P. Michalak, K. Szczotka, Polish heat pump market between 2000 and 2013: European background, current state and development prospects, Renewable and Sustainable Energy Reviews 48 (2015) 791–812. doi:10.1016/j.rser.2015.04.005.
URL `http://www.sciencedirect.com/science/article/pii/S1364032115002750`

[4] I. Verhaert, R. Baetens, F. Van Riet, Performance evaluation of different micro-CHP configurations in real life conditions and the influence of part load behaviour (accepted for proceedings), in: Clima 2019, 2019.

[5] M. G. Nielsen, J. M. Morales, M. Zugno, T. E. Pedersen, H. Madsen, Economic valuation of heat pumps and electric boilers in the Danish energy system, Applied Energy 167 (2016) 189–200. doi:10.1016/J.APENERGY.2015.08.115.
URL `https://www.sciencedirect.com/science/article/pii/S030626191501051X#b0195`

[6] A. Gimelli, M. Muccillo, R. Sannino, Optimal design of modular cogeneration plants for hospital facilities and robustness evaluation of the results, Energy Conversion and Management 134 (2017) 20–31. doi:10.1016/J.ENCONMAN.2016.12.027.
URL `https://www.sciencedirect.com/science/article/pii/S019689041631113X?dgcid=raven_sd_recommender_email#f0025`

[7] H. I. Onovwiona, V. I. Ugursal, Residential cogeneration systems: Review of the current technology, Renewable and Sustainable Energy Reviews 10 (5) (2006) 389–431. doi:10.1016/j.rser.2004.07.005.

[8] H. Al Moussawi, F. Fardoun, H. Louahlia-Gualous, Review of tri-generation technologies: Design evaluation, optimization, decision-making, and selection approach, Energy Conversion and Management 120 (2016) 157–196. doi:10.1016/j.enconman.2016.04.085.
URL `https://www.sciencedirect.com/science/article/pii/S0196890416303375`

[9] A. Mustafa Omer, Ground-source heat pumps systems and applications, Renewable and Sustainable Energy Reviews 12 (2) (2008) 344–371. doi:10.1016/j.rser.2006.10.003.
URL `http://www.sciencedirect.com/science/article/pii/S1364032106001249`

[10] S. J. Self, B. V. Reddy, M. A. Rosen, Geothermal heat pump systems: Status review and comparison with other heating options, Applied Energy 101 (2013) 341–348. doi:10.1016/J.APENERGY.2012.01.048.
URL `https://www.sciencedirect.com/science/article/pii/S0306261912000542`

[11] H. Ren, W. Gao, Y. Ruan, Optimal sizing for residential CHP system, Applied Thermal Engineering 28 (5-6) (2008) 514–523. doi:10.1016/j.applthermaleng.2007.05.001.
URL `http://www.sciencedirect.com/science/article/pii/S1359431107001810`

[12] S. Hackel, A. Pertzborn, Effective design and operation of hybrid ground-source heat pumps: Three case studies, Energy and Buildings 43 (12) (2011) 3497–3504.
[13] C. Di Perna, G. Magri, G. Giuliani, G. Serenelli, Experimental assessment and dynamic analysis of a hybrid generator composed of an air source heat pump coupled with a condensing gas boiler in a residential building, Applied Thermal Engineering 76 (2015) 86–97.
[14] Isso, ISSO 96: Ontwerp, realisatie en beheer van WKK-installaties in utiliteitsgebouwen (in Dutch), 2012.
[15] ASHRAE, Combined heat and power design guide, 2015.
[16] CogenVlaanderen, WKK-Wegwijzer (in Dutch), 2017.
[17] Isso, Handboek integraal ontwerpen van warmtepompinstallaties voor utiliteitsgebouwen (in Dutch), 2007.
[18] Isso, Handboek integraal ontwerpen van collectieve installaties met warmtepompen in de woningbouw (in Dutch), 2007.
[19] D. Haeseldonckx, L. Peeters, L. Helsen, W. D'haeseleer, The impact of thermal storage on the operational behaviour of residential CHP facilities and the overall CO2 emissions, Renewable and Sustainable Energy Reviews 11 (6) (2007) 1227–1243. doi:10.1016/j.rser.2005.09.004.
URL http://www.sciencedirect.com/science/article/pii/S1364032105001036
[20] Z. Beihong, L. Weiding, An optimal sizing method for cogeneration plants, Energy and Buildings 38 (3) (2006) 189–195. doi:10.1016/j.enbuild.2005.05.009.
[21] O. a. Shaneb, G. Coates, P. C. Taylor, Sizing of residential μcHP systems, Energy and Buildings 43 (8) (2011) 1991–2001. doi:10.1016/j.enbuild.2011.04.005.
[22] E. Barbieri, Y. Dai, M. Morini, M. Pinelli, P. Spina, P. Sun, R. Wang, Optimal sizing of a multi-source energy plant for power heat and cooling generation, Applied Thermal Engineering 71 (2) (2014) 736–750. doi:10.1016/j.applthermaleng.2013.11.022.
URL http://www.sciencedirect.com/science/article/pii/S1359431113008119
[23] L. F. Fuentes-Cortés, J. M. Ponce-Ortega, F. Nápoles-Rivera, M. Serna-González, M. M. El-Halwagi, Optimal design of integrated CHP systems for housing complexes, Energy Conversion and Management 99 (2015) 252–263. doi:10.1016/j.enconman.2015.04.036.
URL http://www.sciencedirect.com/science/article/pii/S0196890415003908
[24] X. Kong, R. Wang, X. Huang, Energy optimization model for a CCHP system with available gas turbines, Applied Thermal Engineering 25 (2-3) (2005) 377–391. doi:10.1016/J.APPLTHERMALENG.2004.06.014.
URL https://www.sciencedirect.com/science/article/pii/S1359431104001784
[25] X. Wang, X. Zhou, L. Li, Optimal Design methods and experimental validation for hybrid ground source heat pump system with gas boiler, Procedia Engineering 205 (2017) 4149–4156. doi:10.1016/J.PROENG.2017.10.159.
URL https://www.sciencedirect.com/science/article/pii/S187770581734715X
[26] F. Li, G. Zheng, Z. Tian, Optimal operation strategy of the hybrid heating system composed of centrifugal heat pumps and gas boilers, Energy and Buildings 58 (2013) 27–36. doi:10.1016/j.enbuild.2012.09.044.
URL http://www.sciencedirect.com/science/article/pii/S0378778812005555
[27] M. L. Ferrari, A. Traverso, M. Pascenti, A. F. Massardo, Plant management tools tested with a small-scale distributed generation laboratory, Energy Conversion and Management 78 (2013) 105–113. doi:10.1016/j.enconman.2013.10.044.
URL http://www.sciencedirect.com/science/article/pii/S0196890413006791
[28] D. Fischer, T. R. Toral, K. Lindberg, B. Wille-Haussmann, H. Madani, Investigation of Thermal Storage Operation Strategies with Heat Pumps in German Multi Family Houses, Energy Procedia 58 (2014) 137–144.
[29] G. Angrisani, M. Canelli, A. Rosato, C. Roselli, M. Sasso, S. Sibilio, Load sharing with a local thermal network fed by a microcogenerator: Thermo-economic optimization by means of dynamic simulations, Applied Thermal Engineering 71 (2) (2014) 628–635. doi:10.1016/j.applthermaleng.2013.09.055.
URL http://www.sciencedirect.com/science/article/pii/S1359431113006893
[30] L. Gasser, S. Flück, M. Kleingries, B. Wellig, Efficiency Improvements of Brine / Water Heat Pumps through Capacity Control, in: 12th IEA Heat Pump Conference 2017, 2017.
[31] B. Baeten, F. Rogiers, L. Helsen, Reduction of heat pump induced peak electricity use and required generation capacity through thermal energy storage and demand response, Applied Energy 195 (2017) 184–195.
[32] D. Rolando, H. Madani, G. Braida, R. Tomasetig, Heat pump system control : the potential improvement based on perfect prediction of weather forecast and user occupancy, 12th IEA Heat Pump Conference 2017 (2017) 1–9.
[33] Service Public de Wollonie; Leefmilieu Brussel;, De geslaagde integratie van een warmtekracht installatie in een stookplaats (Dutch).
[34] J. Glembin, M. Adam, J. Deidert, K. Jagnow, G. Rockendorf, H. P. Wirth, Simulation and Evaluation of Different Boiler Implementations and Configurations in Solar Thermal Combi Systems, Energy Procedia 30 (2012) 601–610. doi:10.1016/j.egypro.2012.11.070.
URL http://www.sciencedirect.com/science/article/pii/S187661021201586X
[35] J. Glembin, T. Haselhorst, J. Steinweg, G. Rockendorf, Simulation and Evaluation of Solar Thermal Combi Systems with Direct Integration of Solar Heat into the Space Heating Loop, Energy Procedia 91 (2016) 450–459. doi:10.1016/J.EGYPRO.2016.06.176.
URL https://www.sciencedirect.com/science/article/pii/S1876610216302740
[36] R. Bonabe De Rouge, P. Picard, P. Stabat, D. Marchio, A comparison of integration solutions for a gas Stirling micro-cogeneration system in residential buildings, in: Climamed conference, 2015.
[37] F. Van Riet, G. Steenackers, I. Verhaert, Design of cogeneration : a case study of an apartment block , Proceedings of the REHVA Annual Meeting Conference Low Carbon Technologies in HVAC, 23 April, 2018, Brussels, Belgium (2018) 1–8.
URL https://anet.be/record/opacirua/c:irua:152185/E%0Ahttps://repository.uantwerpen.be/docman/iruaauth/84a81e/152185.pdf

[38] F. Van Riet, E. Janssen, G. Steenackers, I. Verhaert, Hydronic design of cogeneration in collective residential heating systems: state-of-the-art, comparison and improvements, Applied Thermal Engineering 148 (2019) 1246–1257.
[39] F. Van Riet, G. Steenackers, I. Verhaert, Hydronic integration of ground-coupled heat pumps in collective heating system of buildings, in: 10th International Conference on System Simulation in Buildings, Vol. 1, 2018.
[40] R. Vandenbulcke, L. Mertens, E. Janssen, A simulation methodology for heat and cold distribution in thermo-hydronic networks, Building Simulation 5 (3) (2012) 203–217. doi:10.1007/s12273-012-0066-7.
[41] VLAIO, Instal 2020 project: Integraal ontwerp van installaties voor sanitair en verwarming (Dutch), VIS 135098 (2014-2018), www.instal2020.be.
[42] M. De Pauw, F. Van Riet, J. De Schutter, S. Binnemans, J. Van Der Veken, I. Verhaert, A methogology to compare collective heating systems with individual heating systems in buildings, in: Proceedings of the REHVA Annual Meeting Conference: Low Carbon Technologies in HVAC (www.rehvam2018atic.eu), no. April, 2018, pp. 1–8.
[43] VLAIO, Productie en distributie van Sanitair warm water: selectie en dimensionering (Dutch), TETRA 120145 (2012-2014), www.tetra-sww.be.
[44] Solar Energy Laboratory Univ. of Wisconsin-Madison, TRNSYS17 Volume 8 Weather Data (2014).
[45] J. Fong, J. Edge, C. Underwood, A. Tindale, S. Potter, Performance of a dynamic distributed element heat emitter model embedded into a third order lumped parameter building model, Applied Thermal Engineering 80 (2015) 279–287. doi:10.1016/j.applthermaleng.2015.01.067.
URL `https://www.sciencedirect.com/science/article/pii/S1359431115000927?via%3Dihub#bib12`
[46] M. M. Gouda, C. P. Underwood, S. Danaher, Modelling the robustness properties of HVAC plant under feedback control, Building Services Engineering Research and Technology 24 (4) (2004) 271–280. doi:10.1191/0143624403bt077oa.
[47] J. Mitchel, Principles of Heating, Ventilation and Air Conditioning in Buildings, John Wiley Sons Inc., 2013.
[48] Solar Energy Laboratory Univ. of Wisconsin-Madison, TRNSYS 17 Mathematical Reference (2017).
[49] F. Van Riet, G. Steenackers, I. Verhaert, A new approach to model transport delay in branched pipes (in press), in: 10th International Conference on System Simulation in Buildings, Vol. 1, 2018, pp. 1–11.
[50] M. Y. Haller†, J. Paavilainen, L. Konersmann, R. Haberl, A. Dröscher, E. Frank, C. Bales, W. Streicher, A unified model for the simulation of oil, gas and biomass space heating boilers for energy estimating purposes. Part I: Model development, Journal of Building Performance Simulation 4 (1) (2010) 1–18. doi:10.1080/19401491003653629.
URL `http://www.tandfonline.com/doi/abs/10.1080/19401491003671944#.VKs0fNLF-So`
[51] M. Y. Haller†, J. Paavilainen, L. Konersmann, R. Haberl, A. Dröscher, E. Frank, C. Bales, W. Streicher, A unified model for the simulation of oil, gas and biomass space heating boilers for energy estimating purposes. Part II: Parameterization and comparison with measurements, Journal of Building Performance Simulation 4 (1) (2010) 1–18. doi:10.1080/19401491003653629.
URL `http://www.tandfonline.com/doi/abs/10.1080/19401491003671944#.VKs0fNLF-So`
[52] R. Vandebulcke, Hydronic Simulation and Optimisation: a simulation based study on the energy efficiency and controllability of hydronic heating systems, Ph.D. thesis, University of Antwerp (2013).
[53] J. Glembin, G. Rockendorf, E. Betram, J. Steinweg, A new easy-to-parameterize boiler model for dynamic simulations, ASHRAE Transactions 119 (PART 1) (2013) 270–292.
[54] R. B. D. Rougé, T. Tirtiaux, P. Picard, P. Stabat, Experimental Analysis of a Gas Micro-Cogeneration Based on Internal Combustion Engine and Calibration of a Dynamic Model for Building Energy Simulation, in: P. K. Heiselberg (Ed.), CLIMA 2016 - proceedings of the 12th REHVA World Congress, Vol. 3, Aalborg University, Department of Civil Engineering, 2016.
[55] S. Tassou, P. Votsis, Transient response and cycling losses of air-to-water heat pump systems, Heat Recovery Systems and CHP 12 (2) (1992) 123–129.
[56] P. Pärisch, O. Mercker, J. Warmuth, R. Tepe, E. Bertram, G. Rockendorf, Investigations and model validation of a ground-coupled heat pump for the combination with solar collectors, Applied Thermal Engineering 62 (2) (2014) 375–381.
[57] E. Fuentes, D. Waddicor, J. Salom, Improvements in the characterization of the efficiency degradation of water-to-water heat pumps under cyclic conditions, Applied Energy 179 (2016) 778–789.
[58] J. Van der Veken, V. De Meulenaer, H. Hens, How Efficient Are Residential Heating Systems ?, in: CLIMA 2005 proceedings, 2005, p. 6.
[59] J. Van der Veken, V. De Meulenaer, G. Verbeeck, H. Hens, IWT-report: Development of Extreme Low Energy and Low Pollution Buildings by Generic Optimization: Energy Simulation of Installation Components, KU Leuven, Tech. rep. (2008).
[60] I. Verhaert, G. Mulder, M. De Paepe, Evaluation of an alkaline fuel cell system as a micro-CHP, Energy Conversion and Management 126 (2016) 434–445.
[61] HERCULES-foundation, Tijdsonderzoek (www.tijdsonderzoek.be/en/Statistics) (2016).
[62] E. Van Kenhove, K. Dinne, A. Janssens, J. Laverge, Overview and comparison of Legionella regulations worldwide, American Journal of Infection Controldoi:10.1016/J.AJIC.2018.10.006.
URL `https://www.sciencedirect.com/science/article/pii/S0196655318309957`
[63] I. Verhaert, B. Bleys, S. Binnemans, E. Janssen, A Methodology to Design Domestic Hot Water Production Systems Based on Tap Patterns, in: Proceedings of the 12th REHVA World Congress (CLIMA), 2016.
[64] F. Van Riet, H. El Khaoui, F. Hulsbosch, G. Steenackers, I. Verhaert, Exploring the novel software Hysopt: a comparison of hydronic heat distribution systems of an apartment building, in: CLIMA 2016 - proceedings of the 12th REHVA World Congress, 2016.
[65] A.-T. Nguyen, S. Reiter, P. Rigo, A review on simulation-based optimization methods applied to building performance analysis, Applied Energy 113 (2014) 1043–1058. doi:10.1016/j.apenergy.2013.08.061.

URL http://www.sciencedirect.com/science/article/pii/S0306261913007058